# Auxin is not asymmetrically distributed in initiating Arabidopsis leaves

**Neha Bhatia[1] and Marcus G. Heisler[1*]**

**Affiliations**

[1]School of Life and Environmental Sciences, University of Sydney, NSW, Australia

*Author for correspondence: Marcus G Heisler (marcus.heisler@sydney.edu.au)

## Abstract

It has been proposed that asymmetric auxin levels within initiating leaves help establish leaf polarity, based in part on observations of the DII auxin sensor. Here we show that the mDII control sensor also exhibits an asymmetry and that according to the ratio-metric auxin sensor R2D2, no obvious asymmetry in auxin exists. Together with other recent findings, our results argue against the importance of auxin asymmetry in establishing leaf polarity.

## Introduction

The leaves of seed plants are usually flat with distinct cell types making up their dorsal (upper) and ventral (lower) tissues. A fundamental question in plant development is how this dorsal-ventral polarity is first specified. Studies based on wounding experiments have suggested the presence of an inductive signal originating from the meristem that promotes dorsal identity in the adaxial (adjacent to the meristem) tissues of the leaf primordium[1,2]. However more recently, it was found that exogenous application of the plant hormone auxin to tomato leaf primordia resulted in the formation of radialized leaves that appeared ventrilized. Hence, relatively high levels of auxin are proposed to promote ventral or inhibit dorsal leaf cell fate[3]. Extending these conclusions, it was also proposed that an asymmetry in the auxin distribution across the leaf adaxial-abaxial axis at leaf initiation acts to help specify leaf polarity during regular development[3]. A critical piece of evidence supporting this latter proposal is that an auxin sensor, the DII[4,5] indicates low levels of auxin in adaxial leaf tissues compared to abaxial tissues at leaf initiation[3]. Hence asymmetries in auxin concentrations between the adaxial and abaxial leaf tissues, as a result of PIN1 mediated auxin transport, are proposed to help establish leaf polarity[3]. Building on this conclusion, a more recent study proposed that low levels of auxin in adaxial tissues are

33 necessary to restrict the expression of the WOX1 and PRS genes to the middle domain,
34 since auxin promotes their expression[6]. Finally, the reported asymmetry in auxin has
35 also been linked to asymmetries in the mechanical properties of leaf tissues and their
36 morphogenesis[7].
37
38 Despite these studies, reason to reassess the role of any asymmetry in auxin in
39 specifying leaf polarity has arisen due to the recent finding that the expression patterns
40 of genes involved in leaf dorsoventrality are already patterned in meristem tissues
41 where leaves originate, with little change occurring to their expression during organ
42 initiation. Hence leaf polarity appears pre-patterned [8]. Furthermore, rather than
43 compromise dorsal cell fate, auxin was found to promote dorsal cell fate by maintaining
44 Class III HD-ZIP expression and repressing KAN1 expression in the adaxial cells of
45 organ primordia[8], which is the opposite of what would be expected according to the
46 auxin asymmetry hypothesis. In addition, Caggiano et al. (2017) also found that
47 exogenous auxin application to young leaf primordia did not influence the spatial
48 pattern of WOX1 and PRS, only the intensity of expression[8]. This also conflicts with
49 the proposal that low levels of auxin are required in adaxial leaf tissues to prevent
50 ectopic WOX1 and PRS expression as previously proposed[6].
51
52 **Results and discussion**
53 Given the concerns listed above, we decided to examine the distribution of auxin during
54 leaf initiation using not only by the DII sensor assessed in previous studies but also, by
55 looking more closely at the expression pattern of the non-auxin degradable mDII auxin
56 sensor control[4] as well as the ratiometric R2D2 auxin sensor[9]. We initially focused on
57 the first two leaves three and four days after stratification (DAS), when these leaves are
58 initiating as well as a day later as they begin to elongate and included the PIN1-GFP
59 marker in our analysis to correlate auxin levels with PIN1 expression and polarity. At
60 3DAS, the expression patterns of REV and KAN1 are already polar within such
61 primordia, although the FIL expression domain at this stage of development is still
62 being refined[8]. Also at this stage, PIN1 is polarized towards the distal tip of leaf
63 primordia but has reversed polarity away from the primordia, towards the meristem, in
64 cells adjacent to the primordia on the adaxial side. According to the ratio-metric auxin
65 sensor R2D2, auxin concentrations were relatively low in adaxial cells of the primordia
66 but also low in abaxial and lateral regions proximally (Fig1-a and d). High levels of

67 auxin were only found in more distal regions towards the tip of the primordia, matching
68 the overall pattern of signal from PIN1-GFP. No obvious asymmetry in signal between
69 the adaxial and abaxial sides of the primordia was observed. This same overall pattern
70 of signal was found in 16 out of 18 leaves that were examined. At 4DAS, the auxin
71 distribution according to the R2D2 sensor was more uniform although higher levels of
72 auxin appeared associated with the vasculature, again correlating with PIN1 expression
73 (n=12/12 leaves) (Fig. 1 g and j).
74
75 As our results using the R2D2 auxin sensor indicate a different auxin distribution
76 compared to that reported previously using the DII marker [3], we next re-examined the
77 pattern of DII auxin sensor expression at the same developmental stages. In contrast to
78 the R2D2 pattern, the DII pattern showed an asymmetry of expression in leaf primordia
79 at 3 DAS, indicating relatively low auxin levels in adaxial primordium cells, as found
80 previously. DII signal appeared strongest in the adaxial epidermis but was also stronger
81 in the adaxial sub-epidermal cell layer compared to abaxial epidermal and sub-
82 epidermal cell layers (Fig.1- b, e and h) (n=18/18 leaves). One day later, although DII
83 signal was still higher in the adaxial cells of the primordia, it started to show a relatively
84 increased expression in the abaxial sub-epidermal layers as well compared to earlier
85 stage (n=13/14 leaves) (Fig1-k). Overall our results using the DII marker are similar to
86 those obtained previously and consistent with the proposal that there are low levels of
87 auxin in the adaxial regions of leaf primordia, in contrast to our results using the R2D2
88 sensor. Given this discrepancy, we next examined the expression of the mDII sensor
89 which is driven by the same 35S promoter as the DII sensor but is not auxin sensitive.
90 Surprisingly we found that, like the DII results, expression of the mDII marker was also
91 higher in the adaxial cells of the primordia (n= 16/16 leaves) (Fig.1-c,f and i). The
92 pattern appeared almost identical to the pattern found using the DII marker except that
93 the mDII marker also showed high levels of expression in the shoot meristem whereas
94 the DII sensor did not (compare Fig1-b and c). The similarity of expression between
95 DII and mDII was also apparent at 4DAS when the leaves had started to elongate (Fig.1-
96 l) (n=14/14 leaves). To verify the auxin sensitivity of the sensors used we imaged
97 seedlings before and after treatment with 5mM NAA and found a strong decrease in
98 DII expression compared to mDII and an increase in the ratio of VENUS compared to
99 tdTomato signal for the R2D2 sensor, consistent with an increase in auxin levels (Figure
100 S1).

101

102 All together these results indicate that the asymmetry in expression found previously
103 for the DII auxin sensor in very young leaf primordia[3] is not due to an asymmetry in
104 auxin levels but rather, likely due to differences in transcription driven by the 35S
105 promoter used to drive both DII and mDII in adaxial compared to abaxial leaf tissues.
106 We note that although a single section showing control expression of mDII in older
107 leaves was cited by Guan et al., (2017)[10], our results show that this information was not
108 adequate for assessing similarities and differences between DII and mDII at early
109 developmental stages. To check whether adaxial expression in leaf primordia is a
110 characteristic common to other reporters driven by the 35S promoter, we also examined
111 the expression of 35S::H2B-mRFP1 and 35S::EGFP-LTI6b which had previously been
112 combined into the same plant line by crossing[11]. Surprisingly the expression patterns
113 for these markers were not only different to the mDII marker but also different to each
114 other with the H2B marker showing stronger expression in the adaxial and abaxial
115 epidermis and the LTI6b marker showing a more uniform pattern (Fig. S2). These
116 results reveal that even when the same promoter is utilized to drive FP (fluorescent
117 protein) expression, distinct differences in intensity patterns can occur *in planta*. This
118 may be due to differences in the position of T-DNA insertion in the genome or
119 differences in the surrounding DNA of the vector used. All together then, our results
120 highlight the importance of using ratio-metric sensors for *in vivo* measurements since
121 otherwise it is difficult to adequately control for differences in signal intensity due to
122 promoter activity or other confounding factors. Finally, while the R2D2 marker utilizes
123 a single transgene to express two distinct FPs from two identical promoters[9], a
124 potentially improved approach to assess auxin levels *in vivo* may be to utilize a single
125 promoter to drive the auxin-dependent degradation domain II from Aux/IAA proteins
126 linked to a tandem fusion of fast and slowly folding FP variants, such as VENUS and
127 mCherry. Such an approach can enable a more direct readout of protein degradation
128 rates[12,13] and therefore potentially improve measurements of relative auxin
129 concentration.

130

131 While our findings are inconsistent with the proposal that asymmetries in the auxin
132 distribution influence leaf polarity[3], pattern WOX/PRS gene expression [6] or regulate
133 tissue mechanics[7], they also leave other observations unexplained. In particular, to
134 understand the apparent ventrilization of leaf primordia in tomato in response to

135 exogenous auxin[3] will require further work in assessing how auxin distribution patterns
136 change in response to exogenous treatments and how auxin is distributed during regular
137 development in tomato, preferentially using a ratio-metric auxin sensor such as R2D2.
138
139 **Methods**
140 **Plant material and growth conditions.**
141 Seeds of the plants expressing *p35S::DII-VENUS* and *p35S::mDII-VENUS* transgenes
142 (*Columbia* ecotype) were obtained from Dr. Teva Vernoux [4]. R2D2 reporter line
143 carrying *pPIN1::PIN1GFP* transgene (*Landsberg* ecotype) has been described
144 previously[9,14]. Seeds were germinated and grown on GM medium (pH-7 with 1M
145 KOH) containing 1% sucrose, 1X Murashige and Skoog salts (Sigma M5524), MES 2-
146 (MN-morpholino)- ethane sulfonic acid (Sigma M2933), 0.8 % Bacto Agar (Difco),
147 1% MS vitamins (Sigma M3900) in long day conditions.
148
149 **Confocal imaging and data analysis**
150 Seedlings aged 3DAS (days after stratification) and 4DAS were dissected as described
151 previously[14]. Dissected seedlings were then oriented appropriately to obtain a view of
152 the young leaves either from above or from the side. Seedlings were imaged live, on a
153 Leica TCS-SP5 upright confocal laser scanning microscope with hybrid detectors
154 (HyDs) using a 25X water objective (N.A 0.95). VENUS was imaged using argon laser
155 (excitation wavelength 514nm) while tdTomato was imaged using a white light laser
156 (excitation wavelength 561 nm). Z-stacks were acquired in a 512x512 pixel format with
157 section spacing of 1μm and line averaging 2.
158
159 Ratio-metric calculations for R2D2 auxin sensor were performed using ImageJ (FIJI,
160 https://fiji.sc) as described previously[14]. All the images were processed using IMARIS
161 9.0.0 (bit-plane). Optical sections (transverse or longitudinal) were reconstructed using
162 orthogonal slicer in IMARIS.
163
164 **Auxin treatment**
165 Seedlings aged 3DAS were dissected imaged and treated with approximately 10μL of
166 5mM NAA (1-Napthaleneacetic acid) solution in water (0.5M stock in 1M KOH) for
167 60 minutes and imaged again with same settings as prior to treatment.

**Acknowledgements**

We thank Associate Professor Mary Byrne for critical feedback on the manuscript. We thank Dr. Teva Vernoux for kindly providing the seeds of plants expressing *p35S::DII-VENUS* and *p35S::mDII-VENUS* transgenes. We also thank Professor Jim Haseloff for kindly providing the seeds of plants expressing *p35S::H2B-mRFP1* and *p35S::EGFP-LTI6b* transgenes.

**References**

1 Sussex, I. M. Morphogenesis in Solanum tuberosum I: experimental investigation of leaf dorsiventrality and orientation in the juvenile shoot. *Phytomorphology* **5**, 286-300 (1955).

2 Reinhardt, D., Frenz, M., Mandel, T. & Kuhlemeier, C. Microsurgical and laser ablation analysis of leaf positioning and dorsoventral patterning in tomato. *Development* **132**, 15-26 (2005).

3 Qi, J. *et al.* Auxin depletion from leaf primordia contributes to organ patterning. *Proc Natl Acad Sci U S A* **111**, 18769-18774, doi:10.1073/pnas.1421878112 (2014).

4 Brunoud, G. *et al.* A novel sensor to map auxin response and distribution at high spatio-temporal resolution. *Nature* **482**, 103-106, doi:10.1038/nature10791 (2012).

5 Vernoux, T. *et al.* The auxin signalling network translates dynamic input into robust patterning at the shoot apex. *Mol Syst Biol* **7**, 508, doi:10.1038/msb.2011.39 (2011).

6 Guan, C. *et al.* Spatial Auxin Signaling Controls Leaf Flattening in Arabidopsis. *Curr Biol* **27**, 2940-2950 e2944, doi:10.1016/j.cub.2017.08.042 (2017).

7 Qi, J. *et al.* Mechanical regulation of organ asymmetry in leaves. *Nat Plants* **3**, 724-733, doi:10.1038/s41477-017-0008-6 (2017).

8 Caggiano, M. P. *et al.* Cell type boundaries organize plant development. *eLife* **6**, doi:10.7554/eLife.27421 (2017).

9 Liao, C. Y. *et al.* Reporters for sensitive and quantitative measurement of auxin response. *Nat Methods* **12**, 207-210, 202 p following 210, doi:10.1038/nmeth.3279 (2015).

10 Wang, Y. *et al.* The Stem Cell Niche in Leaf Axils Is Established by Auxin and Cytokinin in Arabidopsis. *Plant Cell* **26**, 2055-2067, doi:10.1105/tpc.114.123083 (2014).

11 Federici, F., Dupuy, L., Laplaze, L., Heisler, M. & Haseloff, J. Integrated genetic and computation methods for in planta cytometry. *Nature Methods* **9**, 483-U104, doi:10.1038/nmeth.1940 (2012).

12 Khmelinskii, A. *et al.* Tandem fluorescent protein timers for in vivo analysis of protein dynamics. *Nat Biotechnol* **30**, 708-714, doi:10.1038/nbt.2281 (2012).

13 Barry, J. D., Dona, E., Gilmour, D. & Huber, W. TimerQuant: a modelling approach to tandem fluorescent timer design and data interpretation for

measuring protein turnover in embryos. *Development* **143**, 174-179, doi:10.1242/dev.125971 (2016).

14 Bhatia, N. *et al.* Auxin Acts through MONOPTEROS to Regulate Plant Cell Polarity and Pattern Phyllotaxis. *Curr Biol* **26**, 3202-3208, doi:10.1016/j.cub.2016.09.044 (2016).

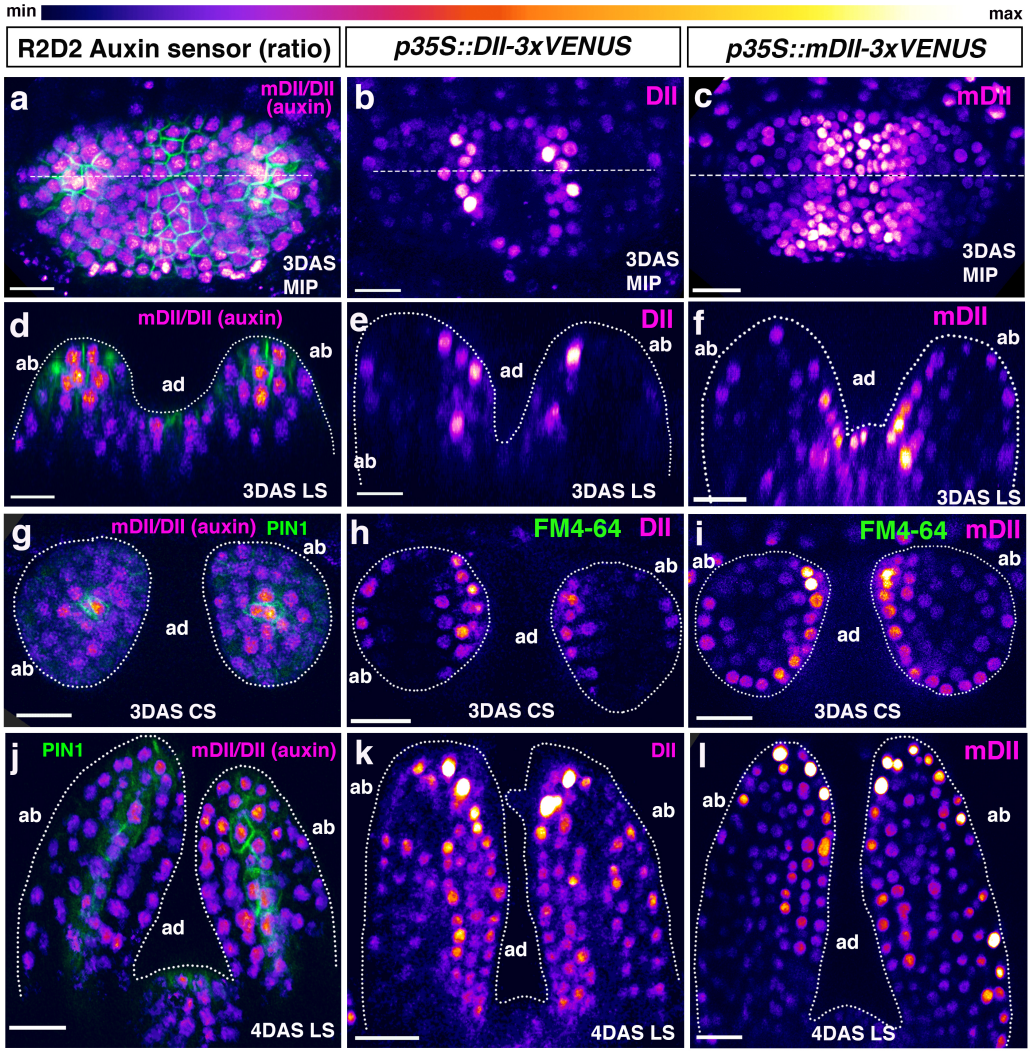


**Figure 1 Predicted auxin distribution in young leaves as indicated by different auxin sensors.**

**(a-c)** Confocal projections of *Arabidopsis* seedlings aged 3DAS (days after stratification) showing predicted auxin distribution based on the ratio-metric auxin sensor R2D2 (magenta) along with PIN1-GFP (green) (a); expression pattern of *p35S::DII-VENUS* (magenta) (b) and *p35S::mutatedDII-VENUS* (mDII, magenta) (c). **(d-f)** Longitudinal reconstructed optical sections of (a-c), respectively, along the dashed lines. **(g-i)** Representative examples of transverse reconstructed optical sections of 3DAS Arabidopsis seedlings showing predicted auxin distribution as indicated by the R2D2 sensor along with PIN1-GFP expression (g), DII-VENUS expression (h) and mDII-VENUS expression (i). R2D2 auxin sensor indicates low but symmetric auxin levels on adaxial and abaxial sides and relatively high auxin levels at the distal tip and in the provasculature where PIN1 expression is also high (d, g). DII-VENUS is more strongly expressed adaxially indicating low auxin levels on the adaxial side of the

238 leaves relative to the abaxial side. However, mDII-VENUS also shows high expression
239 on the adaxial side of the leaf (compare e, h with f, i) and in the shoot meristem. **(j-l)**
240 Representative examples of longitudinal reconstructed optical sections of 4DAS
241 Arabidopsis seedlings showing predicted auxin distribution by R2D2 sensor along with
242 PIN1-GFP expression (green) (i), DII-VENUS expression (j) and mDII-VENUS
243 expression (k). At this stage, the R2D2 sensor indicates a more uniform auxin
244 distribution in the leaf but higher auxin levels in the vasculature where PIN1-GFP
245 expression is also high (j). DII-VENUS shows slightly high expression in adaxial cells
246 and an absence of expression in the vasculature (k). mDII-VENUS shows a similar
247 pattern to DII but is also expressed in the vasculature (l). Scale bars 15μm (a-i) and
248 20μm (j-l).
249

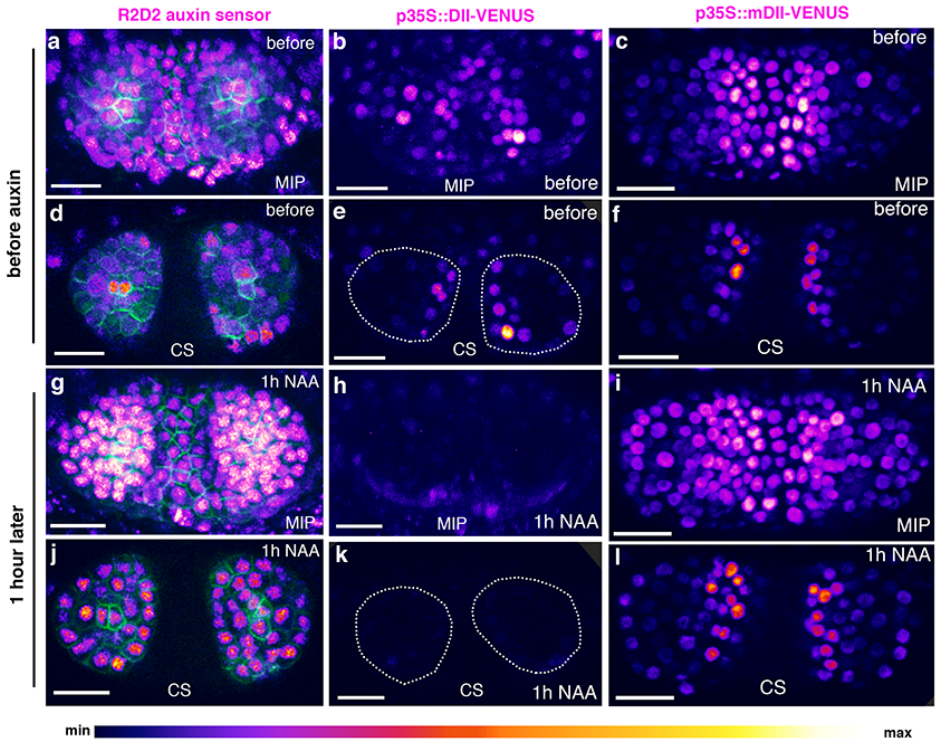


250

251 **Figure S1 Response of different auxin sensors to external auxin application**

252

253 **(a-f)** Confocal projections (a-c) and transverse optical reconstructions (d-f) of
254 *Arabidopsis* seedlings, 3DAS, showing predicted auxin distribution based on R2D2
255 ratio-metric sensor (magenta) along with PIN1-GFP expression in green (a,d), DII-
256 VENUS sensor (magenta) (b,e) and mDII-VENUS sensor (magenta) (c, f) before auxin
257 application. **(g-l)** Confocal projections (g-i) and transverse optical reconstructions (j-l)
258 of *Arabidopsis* seedlings, 3DAS, showing predicted auxin distribution based on R2D2
259 ratio-metric sensor (magenta) along with PIN1-GFP expression in green (a,d), DII-
260 VENUS sensor (magenta) (b,e) and mDII-VENUS sensor (magenta) (c, f) 1hour after
261 the application of 5mM NAA. Note, R2D2 sensor indicates an increased and
262 broadening of auxin levels after NAA application (compare d and j) (n=3/3).
263 Consistently, DII-VENUS shows an attenuated expression within 1 hour of auxin
264 application (compare b,e with h,j) (n=4/4). mDII-VENUS levels do not decrease upon
265 auxin application (compare c,f with i,l) (n=4/4). Scale bars 20µm (a-l).

266

267 Figure S2

268

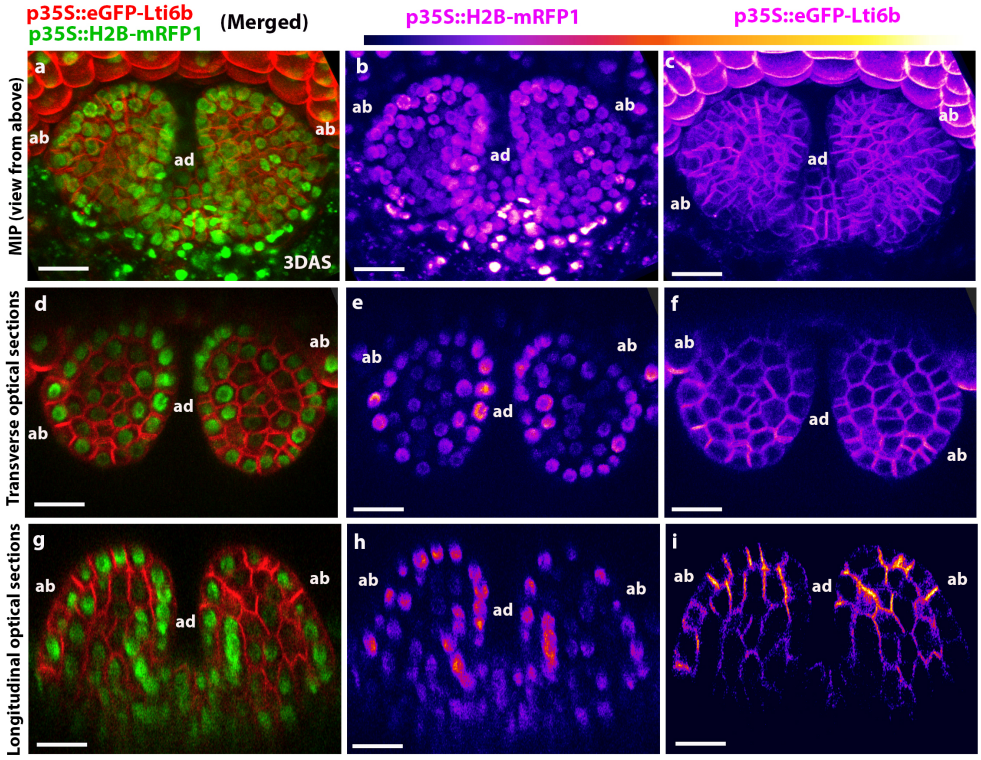


269

270

271 **Figure S2**

272

273 **Different 35S promoter-driven reporter genes show different expression patterns**
274 **in young leaves.**

275

276 **(a-c)** Confocal projections of *Arabidopsis* seedlings aged 3DAS showing expression
277 patterns of a *p35S:eGFP-Lti6b* (membrane marker, green) and *p35S::H2B-*
278 *mRFP1*(nuclear marker red) together (a), *p35S::H2B-mRFP1* only (magenta) (b) and
279 *p35S:eGFP-Lti6b* only (magenta) (c). **(d-f)** Transverse optical reconstructions of (a-c)
280 respectively; merged (d), *p35S::H2B-mRFP1* only (magenta) (e) and *p35S:eGFP-Lti6b*
281 only (magenta) (f). **(g-i)** Longitudinal optical reconstruction of (a-c) respectively;
282 merged (g), *p35S::H2B-mRFP1* only (magenta) (h) and *p35S:eGFP-Lti6b* only
283 (magenta) (i). Note *p35S::H2B-mRFP1* shows similarly high levels of expression in
284 both adaxial (ad) as well as abaxial (ab) epidermal cell layers and weaker expression in
285 the middle regions (e and h). However, *p35S:eGFP-Lti6b* shows no consistent

286 asymmetry in expression throughout the leaf (f and i). Scale bars 20μm (a-i), (n=10
287 leaves).
288